Evaluation of a bio-socially inspired secure DSA scheme using testbed-calibrated hybrid simulations

Anna Wisniewska
Computer Science
Washington State University Vancouver
Vancouver, WA
anna.wisniewska@wsu.edu

Nirnimesh Ghose
School of Computing
University of Nebraska–Lincoln
Lincoln, NE
nghose@unl.edu

Bilal Khan
Department of Sociology
University of Nebraska–Lincoln
Lincoln, NE
bkhan2@unl.edu

***Abstract*—The ongoing explosion of embedded wireless capabilities in contemporary systems has made the availability of wireless spectrum insufficient. The proposed solution to this problem is dynamic spectrum access (DSA) technology where wireless devices (secondary users) opportunistically forage for unused spectrum (for example, TV whitespace and 3.5GHz bands) arising when the licensed users are idle. We put forward a novel bio-social protocol for DSA networks in which the secondary users forage for bands with low contention. The SUs estimate utilization using a novel wireless physical layer signature method to provide security against rogue nodes that seek to benefit by injecting spoofed traffic on behalf of other SUs. We report on the system performance of this formally specified model of bio-social behavior, using simulations that are parameterized by hardware testbed measurements. The results show that a more accurate estimation of band contention improves the efficiency of resource utilization. More broadly, the findings point to the importance of biosocial paradigms in the design of distributed leaderless resource sharing schemes for the wireless ecosystem.**

***Index Terms*—Dynamic spectrum access, bio-social networking, cognitive radio networks, Internet of Things, contention-sensing.**

I. Introduction

The widespread embedding of wireless communication capabilities is impacting systems across many domains like home automation, industrial automation, agricultural automation, and national security automation. This dramatic ongoing shift has led to a shortage of wireless bands relative to the co-existing wireless systems that consume them. The shortage can be tackled by using vacant wireless bands (e.g. TV whitespace and 3.5GHz bands) in different localities, as proposed in the Dynamic Spectrum Access (DSA) paradigm. In DSA, during the absence of a licensed or primary user of a wireless band (e.g. TV broadcast on 400-600MHz or satellite communications on 3.5 GHz), unlicensed users or secondary users (SUs) can make use of bands. Faced with increasingly denser deployments of independent DSA networks that lack a coordination framework, constituent SUs find themselves competing over limited resources of varying characteristics. While the FCC's open access paradigm "allows unlimited numbers of unlicensed users to share frequencies", it "does not provide any right to protection from interference." Channel scarcity, usage dynamism, and "no right of protection from interference" poses self-coexistence and performance challenges for secondary users. The root cause of the problem is a major focus on preserving the interest of the primary user in secondary-primary user interaction. There has been very little focus on studying the SU-SU interaction paradigm.

The current research on resource allocation in wireless communication has been inspired by the co-use of resources in animal and human populations [1], [2]. State-of-the-art has modeled communication resource allocation after the foraging strategies of animal societies [1]–[6]. The autonomous and intelligent SUs in the dynamic spectrum access environment are capable of learning, sensing, and adapting to the dynamic environment. Thus, SUs may evolve much as biological systems have while competing over limited resources.

In previous work, the authors defined a bio-inspired foraging behavioral model for cognitive radio communication where secondary users stochastically transition between a foraging (idle) state and consume (transmitting) state [5], [6]. This idea is orthogonal to previous works where the secondary users are always transmitting [1]–[4]). The authors showed how *social deference*, where a secondary user chooses to stop consuming a band prior to transmitting all of its buffered data to defer to co-users, may achieve fairness in utilization [6]. The authors defined a social contention avoidance behavior model, where secondary users determine the contention in a band before deciding to transmit, significantly improving channel utilization.

In this work, we extend the bio-social model by leveraging unforgeable wireless physical layer sensing of co-users in a band. More specifically, we extend our previous behavioral model by incorporating *imperfect "real-world" knowledge* about band contention as compared to the assumption of instantaneous perfect knowledge of the band of interest (BoI) occupancy level in [5]. We then investigate the performance of the contention-sensing model by comparing it to a behavioral model where SUs are indifferent to band contention. Furthermore, the previous work assumed MAC / Physical address for packet sniffing to determine contention in the band [5]. However, this opens up the security challenge where misbehaving SUs can spoof the addresses to skew the occupancy level estimation of co-existing SUs to gain an

978-1-6654-0066-4/21/$31.00 ©2021 IEEE

unfair share of band usage. To tackle such a misbehaving SU, in this work, we propose a novel technique of utilizing *wireless physical (PHY) layer signatures* for estimating band usage. Specifically, we propose to utilize the received signal strength (RSS) to count the number of SU in the band. The SU estimates the usage of the band by observing the level of RSS and comparing it with previously observed RSS with acceptable errors. The main advantage of utilizing RSS is the fast detection of SUs, occurring within a few starting samples of transmission. We collected the band utilization data on a USRP testbed and compute a curve for the probability of detection. The probability detection function is then utilized in the resource allocation algorithm derived from the resource conflict/sharing in a social setting. We show that SUs with the ability to estimate band contention levels using RSS detection have a performance advantage over SUs without such an ability.

II. Baseline Model (BM) of Biosocial Behavior

For the baseline model (following [5]), we propose to utilize a discrete time stochastic process with n secondary users $S = \{s_1, s_2, ..., s_n\}$ competing over m orthogonal spectrum bands $B = \{b_1, b_2, ..., b_m\}$. The secondary users operate according to the finite state machine (FSM) in Fig. 1. **Although all SUs run the same 2-state FSM, arc transition probabilities vary dynamically over time, and non-uniformly across SUs, based on each individuals' stochastic estimate of the true dynamic channel occupancy.**

The finite state machine has two discrete states $Q = \{q_c, q_f\}$ and a state variable, the band of interest (BoI), which takes on different values $b \in B$ over time. Two time-varying functions, $\alpha_t : S \to B$ and $\gamma_t : S \to \{q_f, q_c\}$, are defined to indicate the BoI and the state of SU s at time t, respectively.

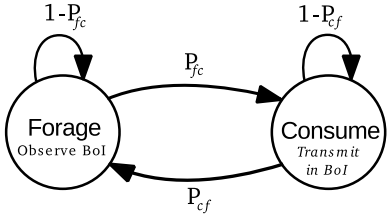

Fig. 1. Finite state machine

If $\alpha_t(s) = b_i$ and $\gamma_t(s) = q_f$, then SU s chooses one of the following at $(t+1)$:

1) With probability P_{fc}, s stays in the band b_i by moving to q_c, i.e. $\alpha_{t+1}(s) = b_i$ and $\gamma_{t+1}(s) = q_c$.
2) With probability $(1 - P_{fc})$, s commits to q_f, i.e. $\alpha_{t+1}(s) = b_j$ and $\gamma_{t+1}(s) = \gamma_t(s)$ $(j \neq i)$ selected uniformly from B.

If $\alpha_t(s) = b_i$ and $\gamma_t(s) = q_c$, then s chooses one of the following $(t+1)$:

1) With probability P_{cf}, s switches to q_f, i.e. $\alpha_{t+1}(s) = b_j$ and $\gamma_{t+1}(s) = q_f$ $(j \neq i)$ selected uniformly from B.
2) With probability $(1 - P_{cf})$, s commits to q_c, using band b_i, i.e. $\alpha_{t+1}(s) = \alpha_t(s)$ and $\gamma_{t+1}(s) = \gamma_t(s)$.

A secondary user is "observing" BoI $b \in B$ in the foraging state q_f. In the consume state q_c, the SU is transmitting in its BoI and receives a reward $R(k)$

$$R(k) = B \cdot log_2 \left(1 + \frac{G_s P_s}{\sum_{i=1}^{k} G_i P_i + \omega}\right) \quad (1)$$

where $k = |\{s' \in S | \alpha_t(s') = \alpha_t(s)\}|$ gives the number of secondary users co-existing in the band, P_s (or P_i) is the transmit power for SU s (or i), G_s is the channel gain of s, B is the bandwidth of the channel, and ω is the ambient white Gaussian noise power level. Equation (1) is consistent with information theoretic modeling used frequently in spectrum sharing literature [7]. To extract the effects of the proposed novel paradigm, we do not include shadowing or pathloss. We assume that all secondary users transmit at the same power level P, experiencing the same channel gain G.

Since an SU s enjoys reward $R(k)$ when it is in the consume state q_c, the reward for all SUs' at a discrete time t is given by

$$W_t = \sum_{i=1}^{m} k_t(i) R(k_t(i)), \quad (2)$$

where the occupancy of the band b is given by $k_t(i) = |\alpha_t^{-1}(i) \cap \gamma_t^{-1}(q_c)|$.

Transmitter reconfigurations are needed when SUs transition to the consume state by re-entering (or entering) the transmission band. This is assumed to be an expensive operation compared to the receiver reconfiguration when switching to q_f. Therefore, in our model, each SU s is charged a fixed cost c for switching bands by transitioning to q_c from q_f. The switching cost for the system at time t is $C_t = c|M_t|$ where c is a constant and

$$M_t = \{s \in S \mid \gamma_{t-1}(s) = q_f \wedge \gamma_t(s) = q_c\} \quad (3)$$

captures the SUs that switched from q_f to q_c at time t. The instantaneous average utility for each SU at t is

$$I_t = \frac{1}{n}(W_t - C_t). \quad (4)$$

The average utility per SU up to time T is

$$U_T = \frac{1}{T} \sum_{t=1}^{T} I_t. \quad (5)$$

In the Baseline Model (BM), SUs transition according to the FSM in Fig. 1 when they have data to transmit. This is modeled by introducing a **system-wide transmission probability parameter** p_x which governs the FSM transitions. Each SU switches from the forage state to the consume state with probability $P_{fc} = p_x$, and from the consume state to the forage state with a probability $P_{cf} = (1 - p_x)$.

III. Detection Model for Channel Co-Use

Now we describe the process of computing the band occupancy level from the hardware testbed data. First, we present the extraction of real-world node detection parameters from

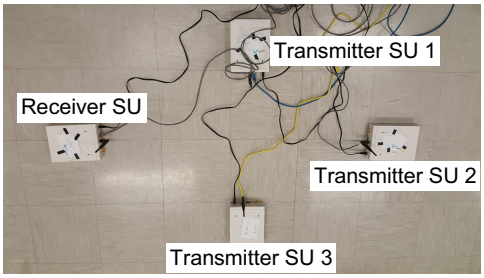

Fig. 2. Setup for capturing real-world data on the USRP platform with three transmitters and one receiver.

the USRP platform. Finally, we present the extraction of the curve from the data, which is the input for the evaluation of the bio-social-inspired model.

A. Collecting Testbed Measurements

We captured the contention function $f(t, n_b, p_x)$ as the holistic effect of varying the number of SUs n_b, and the system-wide transmission probability p_x with time t. Further, we implemented *fast-detection* at the SUs using PHY-layer characteristics to pinpoint the number of active SUs in a particular band. The motivation of using PHY-layer as compared to MAC addresses is that detection can be made within the first few samples received in contrast to extracting MAC address after receiving the whole frame. The PHY-layer characteristics candidates can be (a) the frequency offset [8], (b) the received signal strength [9], (c) the In-phase and quadrature components origin offset [10], (d) the channel impulse response [11], (e) the angle of arrival for the incoming signal [12], and (f) the transient radio state [13]. Some of these proposed methods are challenging to implement for fast detection. The techniques utilizing I/Q origin offset, channel impulse response, and frequency offset require reception of the complete preamble before making the detection. The AOA parameter requires the detector to be capable of very narrow antenna beams when the SUs are close to each other. Such narrow beams can be implemented by a parabolic antenna [14], or by utilizing an antenna array [15]. In either of the cases the hardware is extremely expensive, such as if two 50ft (2.45GHz center frequency) away SUs are separated by 4ft, the base station will need 50-element antenna arrays to perform detection using a line-of-sight path. Therefore, for the fast-detection strategy, we implement a received signal strength (RSS) strategy. In this strategy, the receiver or the detector SU marked received frames from different SUs, if they are received at different RSS. This is under the assumption that the transmitting SUs are transmitting at the same power and are separated by enough distance such that the channel from the transmitter to the receiver is sufficiently different [16].

1) Setup: To evaluate the band occupancy level, we placed three USRP devices acting as the transmitting SUs in our indoor laboratory. The SU received was implemented by another USRP device placed 4ft away from the transmitters. The transmitters were set to transmit at 20dBm, with 100 samples long frame with 1ms symbol duration. The devices were synchronized in time and center frequency of 2.45GHz.

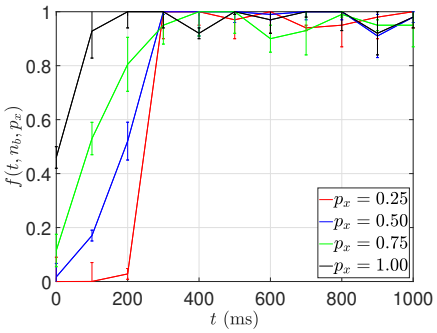

Fig. 3. Detection probability $f(t, n_b, p_x)$ with varying time when number of nodes are fixed to 3.

The SUs transmitted their data according to time division multiple access and selected to transmit in the assigned slot according to p_x. The sampling frequency was set to 2MHz. The experimental setup is shown in Fig 2.

2) Data Captured: During the experiment, we captured the I/Q data using LabView and performed the signal processing on MATLAB [17]. To perform fast detection, we averaged the power of the first 20 samples corresponding to 10 symbols. The receiver marked the frame as received from a new node if the power received differed from previously received powers by 5%. Formally, the receiver used the following equation to count the number of nodes.

$$n = \begin{pmatrix} n_b + 1 \\ \mathbf{P} \cup \{P_t\} \end{pmatrix} \text{ when } P_t \notin \mathbf{P} \ \forall \ t = \{0, \ldots, T\}, \quad (6)$$

where n_b is the number of SUs, P_t is the average power of first 20 samples starting at time t, and T is the total time.

We performed simulation with the experimental data as the ground truth to generate data for the number of SUs $n_b = 5, 7, 10$. In the post-processing we captured the band occupancy level $f(t, n_b, p_x)$ as the fraction of the detected number of SUs and the actual number of SUs present in the band. Figure 3 shows the detection probability with increasing time when we fixed the actual number of SUs to 3 and varied the individual transmission probability. In Fig. 4, we show the detection probability with increasing time when we fixed the individual transmission probability to 0.75 and varied the number of SUs. From the plots, we observe that the detection probability increases with increasing time, and eventually all the nodes are detected. We see this behavior because of the TDMA followed by the nodes.

B. Modeling the testbed data

In the experiment, we captured a total of 3 million data points. We utilized a regression model to fit a curve to the data [18]. We start the derivation of the curve from the plots in Fig. 3. In the plots, we observed the range $f(\cdot)$ is $[0, 1]$ with maximum slope of α/π, and takes the central value at $t = C$, where $C \propto {}^{n_b}/_{p_x}$ and $\alpha \propto {}^{1}/_{n_b \cdot p_x}$. This gives

$$f(t, C, \alpha) = \frac{1}{\pi} \left[\text{atan} \left(\alpha \cdot (t - C) \right) + \frac{\pi}{2} \right]. \quad (7)$$

From Fig. 3 we observed that the individual the system wide transmission probability p_x is inversely proportional to C and

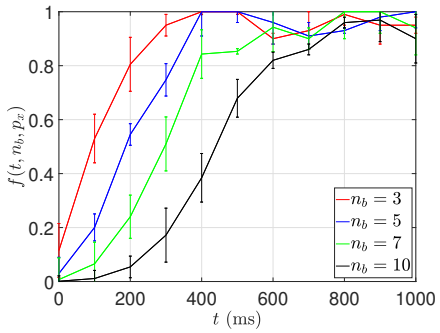

Fig. 4. Detection probability $f(t, n_b, p_x)$ with varying time when transmission probability of each node is fixed to 0.75.

α. Further, from Fig. 4 we observed that the number of nodes n_b is directly proportional to C and inversely proportional to α. Combining these two observations, (7) takes central value when $t = {}^{\mu_1 \cdot n_b}/_{p_x}$ with a slope ${}^{\mu_1}/_{n_b \cdot p_x \cdot \pi}$. Thus we can re-write (7) as

$$f(t, n_b, p_x) = \frac{1}{\pi}\left[\text{atan}\left(\frac{\mu_2 \cdot t}{n_b \cdot p_x} - \frac{\mu_1 \cdot \mu_2}{p_x^2}\right) + \frac{\pi}{2}\right]. \quad (8)$$

Now, we learn the values of μ_1 and μ_2 from the curve fitting function on MATLAB with the data collected from the experiments. We estimated values of $\mu_1 = 24.095$ with 0.0033 standard error and 8.76×10^{-18} p-value and $\mu_2 = 0.070$ with 0.000088 standard error and 7.19×10^{-22} p-value. The estimated values are significant as the p-value is less than 0.05. We now utilize this curve as the input for the bio-social model developed to evaluate the performance.

IV. Combining the Baseline & Detection Models

In this section, we enable SUs to perform contention sensing in bands to enhance the baseline model described in Section II. We extend our previous model [5] by incorporating the USRP testbed data presented in Section III to achieve a realistic model with respect to contention sensing. The extension affects both the FSM transition probabilities and the BoI switching mechanism as described next.

SUs operates according to the finite state machine, as shown in Figure 1. In the contention-sensing model (CSM), an SU has the ability to determine whether the occupancy level in the band is high or low. This is achieved by utilizing a fixed system-wide **band contention threshold parameter** τ. When an SU is consuming band $\alpha_t(s) = b$ while in the q_c state:

1) The probability of switching from q_c to q_f increases to $P_{cf} = p_c + \epsilon$ if $k_t(b) > \tau$ (band occupancy is high).
2) The probability of switching from q_c to q_f decreases to $P_{cf} = p_c - \epsilon$ if $k_t(b) \leqslant \tau$ (band occupancy is low).

When an SU is observing band $\alpha_t(s) = b$ while in the q_f state:

1) The probability of switching from q_f to q_c increases to $P_{fc} = p_f + \epsilon$ if $k_t(b) \leqslant \tau$ (band occupancy is low).
2) The probability of switching from q_f to q_c decreases to $P_{fc} = p_f - \epsilon$ if $k_t(b) > \tau$ (band occupancy is high),

where p_f and p_c were determined in our previous work [5] to maximize utility and used here to facilitate comparison. The selection of the **contention bias parameter** ϵ assists to regulate how sensitive secondary users are towards the chance of contention with other SUs in bands and must satisfy $0 \leqslant \epsilon \leqslant min(p_c, p_f)$. If τ is low, or ϵ is high, SUs will be less tolerant to contention and spend more time looking for low occupancy bands; they will also be equally hesitant to leave low occupancy bands.

As in the baseline model, each SU operates according to the system-wide transmission probability p_x. If an SU has data to transmit in the output buffer, it will determine the contention using function $f(t, n_b, p_x)$ (Eq. 8) where t is the time spent in the current BoI, n_b is the number of SUs in the BoI, and p_x is the system wide transmission probability. When an SU estimates the band occupancy level, it follows the procedure described above to transition between states in the FSM. More specifically, when an SU is in state q_f, the transition probability

$$P_{fc} = p_x \cdot f(t, n_b, p_x) \cdot (p_f + \epsilon)$$

when occupancy is low $(k_t(b) \leqslant \tau)$ and

$$P_{fc} = p_x \cdot f(t, n_b, p_x) \cdot (p_f - \epsilon)$$

when occupancy is high $(k_t(b) > \tau)$. When an SU is in state q_c, the transition probability

$$P_{cf} = p_x \cdot f(t, n_b, p_x) \cdot (p_c + \epsilon)$$

when occupancy is high $(k_t(b) > \tau)$ and

$$P_{cf} = p_x \cdot f(t, n_b, p_x) \cdot (p_c - \epsilon)$$

when occupancy is low $(k_t(b) \leqslant \tau)$.

When an SU is in the forage state q_f, it decides whether to switch to a different BoI. Based on the occupancy level detection probability function $f(\cdot)$, SUs in the contention-sensing population must remain in their BoI for a significant period of time to accurately detect band occupancy. The BoI switching procedure is augmented to depend both on the detection probability $f(\cdot)$ and the contention in the band. If an SU is in the forage state q_f, it will switch bands with probability $f(\cdot)$ only if occupancy is high $(k_t(b) > \tau)$. In other words, an SU will switch bands when it has estimated the occupancy and determined that the contention in the band is too high.

V. Experimental Evaluations

We utilize a probabilistic discrete event simulator to compute utility measurements for various SU societies over time. SUs move according to the FSM in Figure 1. To facilitate comparison with previous results, we use the same parameters as in [6] listed in Table V.

We begin by comparing utility U_T of the contention-sensing society versus the baseline society. In Fig. 5, the x-axis varies transmission probability p_x while the y-axis shows the utility obtained by the baseline and the contention-sensing societies with varying τ. The contention-sensing scheme outperforms the baseline society for all values $p_x < 0.97$. Regardless of the

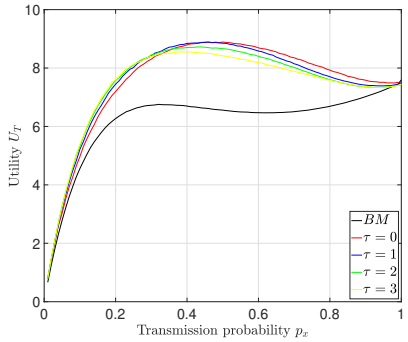

Fig. 5. Utility U_T over transmission probability p_x

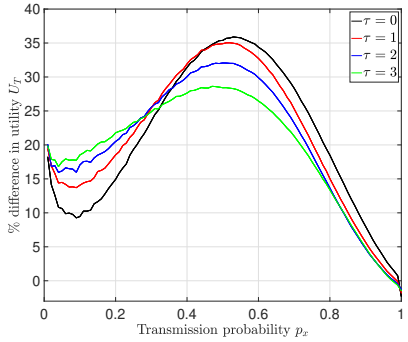

Fig. 6. Percentage difference in utility U_T over transmission prob. p_x

contention threshold τ, the most significant difference in utility U_T between the contention-sensing and baseline societies, occurs for intermediate values of p_x. Figure 6 shows U_T the percentage difference in utility obtained by the contention-sensing population (for different values of contention threshold τ), normalized over the utility acquired by the baseline model. The contention-sensing society enjoys up to a 35% increase in utility when compared to the baseline model. The insignificant advantage when the transmission probability $p_x > 0.97$ is due to the influence of p_x on the FSM transition probabilities. For example, when $p_x = 0.99$ the transition probability from the consume state to the forage state becomes very small (since $1 - p_x = 0.01$) and SUs stay in their bands for extended periods of time. When the transmission probability is very high, the consume-to-forage transition probability is governed by p_x and the contention sensing mechanism has little to no

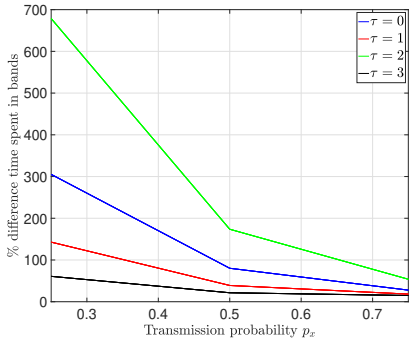

Fig. 7. $\%$ diff. time in band over trans. prob. $p_x = \{0.25, 0.5, 0.75\}$

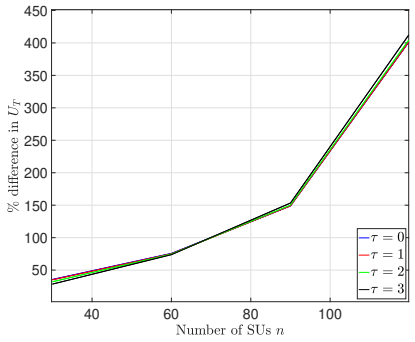

Fig. 8. Percentage difference in utility over n

TABLE I
PARAMETERS FOR BASELINE MODEL

Parameter	Description	Value
m	Number of bands	5
n	Number of SUs	30
P_s	Transmission power of node s	4 W
B	Capacity per band	20 MHz
c	Cost of transmitter reconfig	30% * B
p_f	q_f to q_c Trans. prob.	0.12
p_c	q_c to q_f Trans. prob.	0.2
ϵ	Contention bias	0.05
τ	Contention threshold	varies
p_x	Transmission probability	varies

effect on the transitions between states.

In the proposed model, SUs do not enjoy instantaneous perfect knowledge of the band occupancy. Instead, SUs estimate the band contention using the detection probability function $f(\cdot)$ derived from the testbed experiments. In Fig. 7, the x-axis varies with transmission probability p_x while the y-axis shows the percentage difference in the average time spent in the BoI per SU in the contention-sensing population (for different values of contention threshold τ), normalized by the average time spent in the BoI per SU in the baseline population. In Fig. 7, there is a significant increase in the average time spent in a BoI for the contention-sensing population when compared to the baseline population. For example, when $p_x = 0.25$ the contention sensing society with comfort threshold $\tau = 1$ spends on average 142% more time in a band than the baseline population. The contention-sensing population experience an increase in the average time spent in the band when p_x is decreasing and the number of SU in the band is increasing (which is consistent with the testbed results). Despite the increase in average time spent in a band due to imperfect knowledge of occupancy level, the contention-sensing model utilizes the bands more efficiently with respect to the utility when compared to the baseline.

In the experiments described above we assumed a fixed population size of $n = 30$. To determine the scalability of the experimental results, we vary the SUs to bands ratio. In Fig. 8, the x-axis varies the number of SUs n, while the y-axis shows the percentage difference in utility U_T obtained by the population (for different values of contention threshold τ), normalized by the utility obtained by the baseline. For example, when the population reaches $n = 90$, the contention-sensing society achieves 10% more utility when compared

to the baseline. Figure 8 shows a significant increase in the difference in utility for the contention-sensing population as the SUs to bands ratio increases. Even with the increased SUs to bands ratio, the contention in a band is governed by the contention-threshold parameter τ, which allows the contention-sensing population to amplify their performance advantage when compared to the baseline model.

Finally, we evaluate the overall performance of the real-world contention-sensing model with respect to contention level detection to our previous contention-sensing model [5]. As discussed above, Fig. 5 shows that (1) the contention-sensing model outperforms the baseline model, (2) the contention-sensing model reaches maximum utility when contention threshold $\tau = 0$, and (3) as population size n increases, there is an increase in the difference in utility between the behavioral models. These results are consistent with our previous work and show that the contention-sensing model has a performance advantage over networks where SUs ignore contention levels in bands. Furthermore, the performance of the model tackles the problem of a misbehaving SU capable of emulating the MAC / physical addresses. The wireless PHY layer signature method ensures fast BoI utilization estimation to improve the performance of the model.

VI. Conclusions

A dense wireless population competing over insufficient resources causes complex co-existence hurdles. Analyzing bio-inspired strategies and the study of animal foraging behavior plays a significant role when undertaking these challenges. In this paper, we considered a bio-social behavioral model where secondary users in DSA networks estimate the contention of a band while foraging for a vacant spectrum band. We implemented USRP hardware-tested data-induced simulation experiments trained in a well-specified precise model to assess the contention-sensing system.

We showed that the contention-sensing scheme provides up to 35% more utility when compared to a behavioral model where SUs are indifferent to the contention in bands. We showed that, even though there is an overhead with respect to time while estimating the contention of a band, the contention-sensing model outperforms the baseline no-sensing model for all settings of $p_x < 0.97$. When the transmission probability is high $p_x < 0.97$, the contention-sensing mechanism has a reduced effect, and performance between the two societies is insignificant. Furthermore, we implemented a wireless physical layer signature method for utilization estimation on a USRP testbed platform. The signature method provides a secure system by tackling rogue SUs capable of spoofing MAC / physical addresses to skew other SUs' estimations.

References

[1] J. Li, H. Zhao, A. S. Hafid, J. Wei, H. Yin, and B. Ren, "A bio-inspired solution to cluster-based distributed spectrum allocation in high-density cognitive internet of things," *IEEE Internet of Things Journal*, vol. 6, no. 6, pp. 9294–9307, 2019.

[2] O. A. Oki, P. Mudali, M. Adigun, and T. O. Olwal, "Using biologically-inspired foraging approach for spectrum reconfiguration in distributed cognitive radio network," in *Proc. of IEEE 5G World Forum (5GWF)*. IEEE, 2018, pp. 488–492.

[3] S. Bitam, A. Mellouk, and S. Zeadally, "Bio-inspired routing algorithms survey for vehicular ad hoc networks," *IEEE Communications Surveys & Tutorials*, vol. 17, no. 2, pp. 843–867, 2014.

[4] F. Goudarzi, H. Asgari, and H. S. Al-Raweshidy, "Traffic-aware vanet routing for city environments—a protocol based on ant colony optimization," *IEEE Systems Journal*, vol. 13, no. 1, pp. 571–581, 2018.

[5] A. Wisniewska and B. Khan, "Contention-sensing and dynamic spectrum co-use in secondary user cognitive radio societies," in *2014 international wireless communications and mobile computing conference (IWCMC)*. IEEE, 2014, pp. 157–162.

[6] A. Wisniewska, B. Khan, A. Al-Fuqaha, K. Dombrowski, and M. A. Shattal, "Social deference and hunger as mechanisms for starvation avoidance in cognitive radio societies," in *Proc. of International Wireless Communications and Mobile Computing Conference (IWCMC)*. IEEE, 2016, pp. 1063–1068.

[7] T. M. Cover and J. A. Thomas, *Elements of Information Theory*. John Wiley & Sons, 2012.

[8] J. Hua, H. Sun, Z. Shen, Z. Qian, and S. Zhong, "Accurate and efficient wireless device fingerprinting using channel state information," in *Proc. of IEEE Conference on Computer Communications*. IEEE, 2018, pp. 1700–1708.

[9] N. Ghose, L. Lazos, and M. Li, "HELP: Helper-enabled in-band device pairing resistant against signal cancellation," in *Proc. of 26th USENIX Security Symposium*, 2017, pp. 433–450.

[10] Y. Ren, L. Peng, W. Bai, and J. Yu, "A practical study of channel influence on radio frequency fingerprint features," in *Proc. of IEEE International Conference on Electronics and Communication Engineering (ICECE)*. IEEE, 2018, pp. 1–7.

[11] F. Adamsky, T. Retunskaia, S. Schiffner, C. Köbel, and T. Engel, "Wlan device fingerprinting using channel state information (CSI)," in *Proc. of ACM Conference on Security & Privacy in Wireless and Mobile Networks*, 2018, pp. 277–278.

[12] R. D. Timoteo and D. C. Cunha, "A scalable fingerprint-based angle-of-arrival machine learning approach for cellular mobile radio localization," *Computer Communications*, vol. 157, pp. 92–101, 2020.

[13] N. Soltanieh, Y. Norouzi, Y. Yang, and N. C. Karmakar, "A review of radio frequency fingerprinting techniques," *IEEE Journal of Radio Frequency Identification*, vol. 4, no. 3, pp. 222–233, 2020.

[14] H. J. Visser, *Array and phased array antenna basics*. John Wiley & Sons, 2006.

[15] V. Rabinovich and N. Alexandrov, "Typical array geometries and basic beam steering methods," in *Antenna Arrays and Automotive Applications*. Springer, 2013, pp. 23–54.

[16] T. S. Rappaport *et al.*, *Wireless communications: principles and practice*. Prentice Hall PTR New Jersey, 1996, vol. 2.

[17] MATLAB, *version 9.9.0.1462360 (R2020b)*. Natick, Massachusetts: The MathWorks Inc., 2020.

[18] W. Dumouchel, F. O'Brien *et al.*, "Integrating a robust option into a multiple regression computing environment," in *Computer science and statistics: Proceedings of the 21st symposium on the interface*. American Statistical Association Alexandria, VA, 1989, pp. 297–302.